Molecular Biology of the Cell
Vol. 19, 4032–4041, October 2008

Glucocorticoid Signaling Defines a Novel Commitment State during Adipogenesis *In Vitro*

Carlos Pantoja, Jason T. Huff, and Keith R. Yamamoto

Department of Cellular and Molecular Pharmacology, University of California, San Francisco, CA 94107-2280

Submitted April 24, 2008; Revised July 3, 2008; Accepted July 10, 2008
Monitoring Editor: Kunxin Luo

Differentiation of 3T3-L1 preadipocytes can be induced by a 2-d treatment with a factor "cocktail" (DIM) containing the synthetic glucocorticoid dexamethasone (dex), insulin, the phosphodiesterase inhibitor methylisobutylxanthine (IBMX) and fetal bovine serum (FBS). We temporally uncoupled the activities of the four DIM components and found that treatment with dex for 48 h followed by IBMX treatment for 48 h was sufficient for adipogenesis, whereas treatment with IBMX followed by dex failed to induce significant differentiation. Similar results were obtained with C3H10T1/2 and primary mesenchymal stem cells. The 3T3-L1 adipocytes differentiated by sequential treatment with dex and IBMX displayed insulin sensitivity equivalent to DIM adipocytes, but had lower sensitivity to ISO-stimulated lipolysis and reduced triglyceride content. The nondifferentiating IBMX–then-dex treatment produced transient expression of adipogenic transcriptional regulatory factors C/EBPβ and C/EBPδ, and little induction of terminal differentiation factors C/EBPα and PPARγ. Moreover, the adipogenesis inhibitor preadipocyte factor-1 (Pref-1) was repressed by DIM or by dex-then-IBMX, but not by IBMX-then-dex treatment. We conclude that glucocorticoids drive preadipocytes to a novel intermediate cellular state, the dex-primed preadipocyte, during adipogenesis in cell culture, and that Pref-1 repression may be a cell fate determinant in preadipocytes.

INTRODUCTION

The ability to store excess energy for future use has been strongly selected during evolution. In mammals, adipocytes comprise a tissue responsible for this function. These cells store excess energy in the form of triglycerides that are contained inside lipid droplets, organelles composed of a neutral lipid core surrounded by a protein-coated single phospholipid layer. Excess adipose tissue is associated with numerous diseases including cancer, diabetes, hypertension, and cardiovascular disease (Ogden *et al.*, 2007). Indeed, it has been established that fat cells, in addition to their role in energy storage, also perform endocrine functions. Adipocytes are intimately involved in metabolic homeostasis by secreting and responding to hormones and cytokines that regulate energy intake and expenditure. Notably, differentially located human fat depots display distinct metabolic characteristics, perhaps accounting for the strong association of excess visceral fat, but not subcutaneous fat, with cardiovascular disease (Funahashi and Matsuzawa, 2007).

The apparent functional distinction between visceral and subcutaneous fat raises the question of whether these cells represent two distinct terminal differentiation fates. Fat depots are thought to arise during development from mesenchymal/mesodermal stem cells (MSC) and neural crest stem cells that differentiate through the process of adipogenesis. Work during the past two decades has identified a large number of signaling pathways (e.g., WNT, bone morphogenetic proteins, fibroblast growth factors, and glucocorticoids) that regulate alternative cell fates of mesodermal lineages (bone, cartilage, muscle, or fat) during development or postnatal periods. Despite this accumulated knowledge, we have no definitive view of mammalian fat ontogenesis (Farmer, 2006; Gesta *et al.*, 2007). Indeed, it is unknown to what degree adipogenesis follows the paradigm established by studies of the hematopoietic system: the hematopoietic stem cell gives rise to distinct lineages through a series of commitment steps mediated by specific signaling events that lead to stereotypic changes in the complement of genes expressed in the committed cell type. The identity of cells within these lineages is defined by distinct cell surface markers and transcriptional regulatory factors. Additionally, the hormones and signals that promote differentiation at each step have been largely determined (Kondo *et al.*, 2003). In contrast, the preadipocyte remains the only described intermediary cellular type during differentiation of adipocytes. Preadipocytes are operationally defined as cells isolated from the stromovascular fraction of fat depots that possess the ability to progress toward an adipocytic cell fate when stimulated with "adipogenic cocktails." Recent studies have begun to define molecular markers specific to preadipocytes (Gesta *et al.*, 2006; Tchkonia *et al.*, 2007). However, we do not know the signals that induce preadipocyte commitment or if there are markers that clearly distinguish preadipocyte populations resident in the various fat depots of mammals. Furthermore, the existence of putative intermediary cellular states between preadipocytes and adipocytes has not been determined. Finally, the rules that govern preadipocyte/MSC differentiation to generate adipocytes with varied metabolic phenotypes remain for the most part unknown.

This article was published online ahead of print in *MBC in Press* (http://www.molbiolcell.org/cgi/doi/10.1091/mbc.E08–04–0420) on July 23, 2008.

Address correspondence to: Keith R. Yamamoto (yamamoto@cmp.ucsf.edu).

Abbreviations used: dex, dexamethasone; IBMX, methylisobutylxanthine; Ins, insulin; FBS, fetal bovine serum; CS, calf serum; MSC, mesenchymal stem cell; ISO, isoproterenol; C/EBP, CCAAT/enhancer-binding protein; PPAR, peroxisome proliferator-activated receptor; Pref-1, preadipocyte factor 1.

Here, we have begun to explore these questions using cell culture models of adipogenesis. The 3T3-L1 cell line is one of the most robust cell culture adipogenesis systems, and its relevance has been repeatedly confirmed in mouse models. 3T3-L1 preadipocytes are normally differentiated into adipocytes by a two-step protocol: First, cells are grown to confluence and maintained for 2 d in a postconfluent state in the presence of medium containing calf serum (CS). Next, cells are exposed for another 2 d to a differentiation cocktail (DIM) that contains the glucocorticoid dexamethasone (dex), the growth factor *i*nsulin, the phosphodiesterase inhibitor methylisobutylxanthine (IBMX) and fetal bovine serum (FBS). This signaling protocol launches a transcriptional cascade that, once initiated, is independent of DIM and culminates in the formation of mature adipocytes after 6–8 d of culture (Otto and Lane, 2005). Terminal differentiation is typically assessed using lipid dyes and by monitoring metabolic activities and gene expression specific to adipocytes.

Individually, some of the components of the DIM cocktail are known to influence adipogenesis in vivo. Repeated injection of insulin for diabetes control, for example, has been shown to induce local adipogenesis at the sites of injection (Fujikura *et al.*, 2005). In addition, excess glucocorticoids are responsible for the excess visceral adipose tissue observed in patients with Cushing's syndrome (Rockall *et al.*, 2003). Finally, the downstream effector of IBMX actions, cAMP, appears to modulate polyunsaturated fatty acid–induced obesity in mice (Madsen *et al.*, 2008). Collectively, these observations suggest that the pathways activated by the DIM cocktail could induce adipogenesis by mechanisms that are potentially separable and independent from one another. In particular, it seemed possible that the signaling pathways activated by DIM treatment could encompass distinct commitment stages in the progression from preadipocyte to adipocyte. To begin to examine this hypothesis, we temporally uncoupled the activities of the four signaling components of the DIM cocktail and determined if sequential treatment might reveal distinct intermediates during preadipocyte differentiation. Furthermore, we sought to identify cellular factors that participate in defining such intermediates.

MATERIALS AND METHODS

Cell Culture Lines and Differentiation

3T3-L1 preadipocytes (ATCC, Manassas VA) were cultured in DMEM with 10% calf serum (Hyclone, Logan UT). C3H10T1/2 cells (UCSF Cell Culture Facility) were cultured in DMEM with 10% FBS (GIBCO, Rockville, MD). Mouse MSCs were obtained from 2- to 3-mo-old mice. The bone marrow was extracted with a 23-gauge needle by flushing the femur marrow cavity with 2 ml Iscove's media supplemented with 2% FBS per bone. Flushed bone marrow was cultured in mesenchymal stem cell enrichment media (StemCell Technologies, Vancouver, BC, Canada). Media was changed daily during 3 d to remove the hematopoietic nonadherent cells and then every other day thereafter. At the appearance of large circular colonies of MSCs, cells were trypsinized and passaged to enrich for MSCs.

Primary bone marrow–derived mesenchymal stem cells, 3T3-L1 preadipocytes, and C3H10T1/2 cells were induced to differentiate by treatment with various combinations of 1–10 μg/ml insulin (UCSF Cell Culture Facility), 0.5 mM 3-isobutyl-1-methylxanthine (Sigma, St. Louis, MO), 1 μM dex (Sigma), and 1 μM rosiglitazone (BioMol, Plymouth Meeting, PA). After treatment, cells were maintained in cell culture medium until processing for analysis.

Insulin-stimulated Glucose Uptake

Day 10 after treatment 3T3-L1 cells cultured in 12-well plates were serum-starved in DME-H21 medium for 4 h. Each treatment group consisted of three wells that were washed with PBS at 37°C and incubated for 10 min with 500 μl of PBS; PBS with insulin (10 μg/ml); or PBS, insulin, and cytochalasin B (20 μM). Next, cells were incubated with 2-deoxyglucose (50 μM) and [^{3}H]2-deoxyglucose (2 μCi/ml) in PBS, for 10 min at 37°C. Reaction was stopped by washing wells with PBS at 4°C. Cells were lysed in 200 μl of 0.1% SDS and combined with 3.5 ml of biodegradable scintillation counting cocktail. [^{3}H]2-deoxyglucose uptake was determined in a multipurpose-scintillation counter (Beckman, Fullerton, CA; LS6500). Insulin-stimulated uptake was determined by calculating the count number ratio of PBS to insulin over the PBS group, after subtraction of nonspecific uptake (cytochalasin B group). We used the two-tailed, unpaired Welch's *t* test, adjusted for multiple tests by Bonferroni correction, to generate p values.

Triglyceride Content Determination

Triglyceride levels of day 10 after treatment cells were measured by colorimetric detection of glycerol produced by triglyceride hydrolysis, according to manufacturer's instructions. Triglyceride assay kit (Zen-Bio, Research Triangle Park, NC; TG-1-NC), We used the two-tailed, unpaired Welch's *t* test, adjusted for multiple tests by Bonferroni correction, to generate p values.

Lipolysis

Lipolysis rates of day 10 after treatment cells were determined by detection of free glycerol release, according to manufacturer's instructions. Cells were exposed to isoproterenol (ISO; 10 μM) or control solvent for 3 h before measurement (lipolysis assay kit LIP-3; Zen-Bio). We used the two-tailed, unpaired Welch's *t* test to generate the p value comparing ISO-induced lipolysis rates for DIM- and dex-then-IBMX–differentiated cells after normalizing each to the mean lipolysis rate without ISO addition.

Oil Red O Staining

3T3-L1 cells were washed three times with PBS and fixed in 10% Formalin in PBS for 1 h. After washing the cells twice with PBS, cells were stained with Oil Red O staining solution (0.5% Oil Red O in isopropanol, diluted 3:2 in water and filtered with a 0.22-μm filter; Sigma). After staining, cells were washed three times with water. Representative images of treated cells were obtained with a Zeiss Axiovert 40 CFL inverted microscope (Thornwood, NY) or by scanning of stained plates (Perfection 2450 photo scanner, Epson, Long Beach, CA). The objectives LD A-Plan 20× and A-Plan 10× were used for microscopy.

Immunoblot

3T3-L1 cells were washed with PBS at 4°C and lysed on RIPA buffer (10 mM Tris-HCl, pH 8.0, 1 mM EDTA, 150 mM NaCl, 5% glycerol, 0.1% sodium deoxycholate, 0.1% SDS, and 1% Triton X-100, supplemented with protease inhibitors) at 4°C. Cell lysates were rotated for 15 min at 4°C and cleared by centrifugation (21,000 × g for 15 min at 4°C). Protein lysates were resolved by SDS-PAGE and transferred to PVDF (Millipore, Bedford, MA) membranes using semidry transfer (Bio-Rad, Richmond, CA). Membranes were blocked for 1 h at 22°C with 5% (wt/vol) nonfat powder milk on TBS-T (10 mM Tris-base, 150 mM NaCl, and 0.1% Tween-20, pH 7.6). Membranes were incubated overnight with primary antibodies in TBS-T, 1% (wt/vol) milk at 4°C, followed by 1 h at 22°C in the presence of secondary antibody in TBS-T 1% (wt/vol) milk. Proteins were detected by chemiluminescence (ECL PLUS Western Blot Detection System, Amersham, Indianapolis, IN). The following antibodies were used: C/EBPδ (sc-151), C/EBPβ (sc-150), C/EBPα (sc-61), PPARγ (sc-7196), preadipocyte factor-1 (Pref-1; sc-8625), actin (sc-1616), and anti-goat IgG-HRP (sc-2020) from Santa Cruz Biotechnology (Santa Cruz, CA) and ECL anti-rabbit IgG-HRP (NA934V) from GE Healthcare (Waukesha, WI).

Microarrays and Quantitative Real-Time PCR

Total RNA was isolated from cells by using QIAshredder and RNeasy kits (Qiagen). For microarray experiments, cDNA was generated by one cycle of reverse transcription (Superscript II, Invitrogen, Carlsbad, CA) using 15 μg of total RNA. Experiments were performed using the Mouse Exonic Evidence-based Oligonucleotide (MEEBO) microarray oligo set. Experimental samples labeled with cy5 were hybridized against cy3-labeled experimental pool samples. Arrays were gridded with SpotReader (Niles Scientific, Portola Valley, CA). Microarray data are available at the Gene Expression Omnibus Web site (http://www.ncbi.nlm.nih.gov/geo/) under accession no. GSE11249. All linear models for differential gene expression were constructed with *limma* (Smyth, 2004) in BioConductor (www.bioconductor.org; Gentleman *et al.*, 2004). Probes were normalized without background subtraction using the "printtiploess" method of *limma* (Smyth and Speed, 2003). A linear model for dex was constructed to compare four biological replicates of mock DMSO treatment with dex treatment at either 2 or 36 h. The single-color DIM time-course data (Burton *et al.*, 2004) were normalized without background subtraction and summarized by Tukey biweight using the "three-step" method of *affyplm* in Bioconductor (Bolstad *et al.*, 2003). A linear model for DIM was constructed to compare the two biological replicates at each time point to the time 0 controls. Genes were considered differentially expressed if at least one probe had log-odds greater than 50:50 in the linear model. Furthermore, overlap of dex and DIM differential expression was for genes differentially expressed both at 2 or 36 h of dex treatment and at some point in the DIM time course and with a fold-change greater than 2 in at least one of the conditions. Gene ontology enrichments were generated using DAVID Bioinformatics Resources 2008 (Dennis *et al.*, 2003).

To generate cDNA for quantitative real-time PCR (qPCR), 1 μg of total RNA, 4 μl of 2.5 mM dNTP, and 2 μl of 15 μM random primers (New England

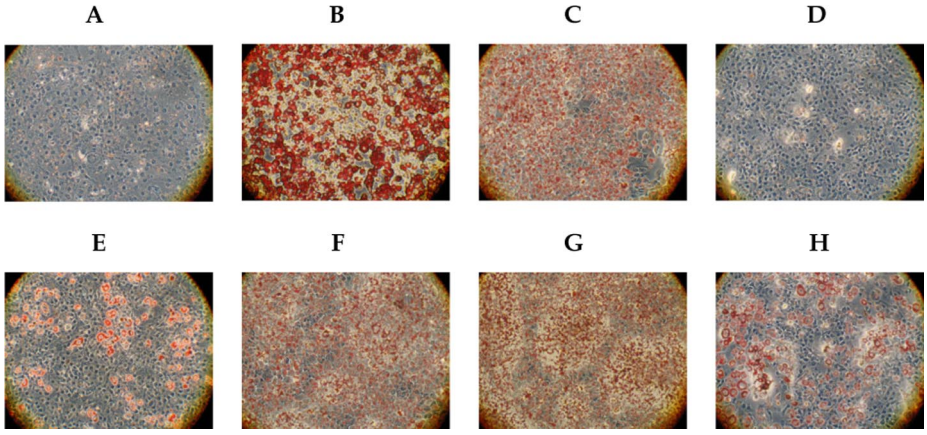

Figure 1. Oil Red O–stained 3T3-L1 cells treated under different differentiation conditions. Two-day confluent 3T3-L1 cells were treated for the indicated times and stained 8 d later with Oil Red O. Cells were observed with light microscopy, 20× magnification. (A) No treatment control. (B) Treatment with DIM (0.5 mM IBMX, 1 μM dex, 1 μg/ml INS, and 10% FBS) for 48 h followed by treatment with INS for 48 h. (C) Treatment with 1 μM dex for 48 h followed by treatment with 0.5 mM IBMX for 48 h. (D) Treatment with 0.5 mM IBMX for 48 h followed by treatment with 1 μM dex for 48 h. (E) Simultaneous treatment with 1 μM dex and 0.5 mM IBMX for 48 h. (F) Treatment with vehicle for 48 h followed by treatment with DIM for 48 h. (G) Treatment with dex for 48 h followed by treatment with DIM for 48 h. (H) Treatment with 0.5 mM IBMX for 48 h followed by treatment with DIM for 48 h.

Biolabs, Beverly, MA) were mixed and incubated at 70°C for 10 min. A 4-μl cocktail containing 25 U of Moloney murine leukemia virus (M-MuLV) Reverse transcriptase (New England Biolabs), 10 U of RNasin (Promega, Madison, WI), and 2 μl of 10× reaction buffer (New England Biolabs) was added and incubated at 42°C for 1 h. The reaction was incubated at 95°C for 5 min. The resultant cDNA was diluted to 100 μl, and 4 μl was used for each 35-μl reaction containing 1.25 U of *Taq* DNA polymerase (Applied Biosystems, Foster City, CA), 1× reaction buffer, 1.5 mM $MgCl_2$, 0.5 mM dNTP (Invitrogen), 0.4× SYBR green I dye (Molecular Probes, Eugene, OR), and 357 nM each primer. qPCR was performed in the 7300 Real-Time PCR System (Applied Biosystems) and analyzed by using the Ct method (7300 System SDS Software, Applied Biosystems). Rpl19 was used as an internal control for data normalization. Primer sequences are available in Supplemental Table S2. qPCR primers for C/EBPα, C/EBPδ, RPL19, Glut4, and Pref-1 were designed using Primer3 (http://frodo.wi.mit.edu/cgi-bin/primer3/primer3_www.cgi). C/EBPβ primer sequences were previously published (Peinnequin *et al.*, 2004). PPARγ primer sequences were obtained from the Nuclear Receptor Signaling Atlas (http://www.nursa.org/).

RESULTS

Effect of Temporal Uncoupling on the Ability of DIM Cocktail Components to Induce Adipogenesis of 3T3-L1 Preadipocytes

To test the hypothesis that components of the DIM cocktail perform distinct and separable actions, we treated postconfluent cells for 48 h with one, two, or three components of DIM followed by treatment with combinations of the remaining factors for another 48 h. We evaluated differentiation levels by staining with the neutral lipid dye Oil Red O.

Surprisingly, we found that the insulin and FBS components of the cocktail were dispensable for complete adipogenesis (>90%) when the 3T3-L1 preadipocytes were treated sequentially, first with dex for 48 h followed by IBMX for 48 h. In contrast, treatment with IBMX followed by dex did not induce significant differentiation (<5%). Most unexpectedly, simultaneous treatment with dex and IBMX for 48 h led to low adipogenesis levels (10–20%). Moreover, pretreatment of 3T3-L1 cells with IBMX rendered preadipocytes partially resistant to differentiation induced by the full DIM cocktail, whereas pretreatment with dex had no such effect (Figure 1).

We conclude from these results that dex and IBMX can induce full adipogenesis by performing actions that are essential and separable, but noncommutative. In addition, the full differentiation observed with dex followed by IBMX treatment, coupled with the reduced differentiation upon simultaneous treatment with dex and IBMX suggests that IBMX action may depend upon a prior process mediated by dex. For example, dex treatment may lead to the accumulation of a product that is needed for IBMX action or it may decrease the levels of an inhibitor of differentiation. Indeed, simultaneous treatment of 3T3-L1 preadipocytes with dex and IBMX for 96 h, instead of 48 h, was capable of inducing full differentiation (Supplemental Figure S1). Thus, when preadipocytes are induced to differentiate with the full DIM cocktail, FBS and insulin might accelerate the kinetics of a rate-limiting step.

Sequential Treatment of C3H10T1/2 and Primary Mesenchymal Stem Cells with Dex and IBMX Induces Adipogenesis

Importantly, the capacity for sequential exposure to dex followed by IBMX to induce adipogenesis is not restricted to 3T3-L1 cells. The mesenchymal stem cell line C3H10T1/2 and primary mouse MSCs, both of which undergo adipogenesis in response to the classic DIM cocktail (Otto and Lane, 2005), also differentiated to adipocytes with sequential dex and IBMX treatment, albeit at lower efficiency than with the full DIM cocktail (Figure 2); conversely, treatment of C3H10T1/2 cells or primary MSCs with IBMX followed by dex failed to induce differentiation. Dex-treated MSCs, however, required insulin to differentiate into adipocytes upon subsequent treatment with IBMX.

These findings indicate that under these circumstances, insulin is required for differentiation of MSCs, but not preadipocytes. Dex, in contrast, is necessary for differentiation of both cell types and provides a signal that primes preadipocytes toward differentiation, but is not sufficient to bring MSCs to the same stage during adipogenesis. These results support the hypothesis that components of the DIM cocktail can perform actions that are discrete and separable. Furthermore, our results are consistent with a model in which glucocorticoids establish a novel cellular intermediate, the "dex-primed preadipocyte," in the progression from preadipocytes toward adipocytes.

Expression Profile of Dex-primed Preadipocytes

We further characterized dex-primed preadipocytes by determining the dose-response and time-course properties of the glucocorticoid signal during priming of 3T3-L1 preadipocytes. We found that complete priming required dex treatment for 36 h and that under these conditions, dex had an EC50 ≅100 nM (Supplemental Figure S2). To examine

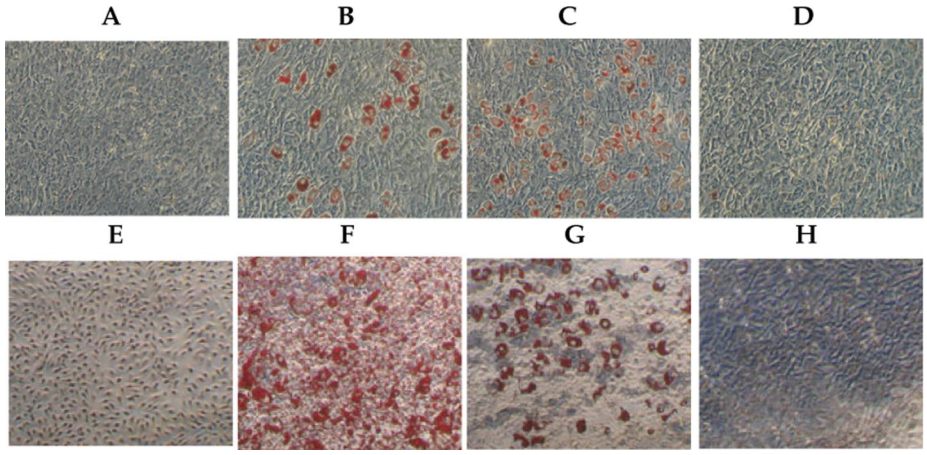

Figure 2. Oil Red O–stained C3HT101/2 and primary mesenchymal stem cells (MSC) cells treated under different differentiation conditions. Two-day confluent C3HT101/2 (A–D) and primary MSCs (E–H) cells were treated for the indicated times and stained 8 d later with Oil Red O. Cells were observed with light microscopy, 20× magnification. (A) Control. (B) Treatment with 0.5 mM IBMX, 1 μM dex, 1 μg/ml INS, and 10% FBS for 48 h followed by 48 h of INS treatment. (C) Treatment with 1 μM dex and 1 μg/ml INS for 48 h followed by 0.5 mM IBMX treatment for 48 h. (D) Treatment with 0.5 mM IBMX and 1 μg/ml INS for 48 h followed by 1 μM dex treatment for 48 h. (E) Control. (F) Treatment with 0.5 mM IBMX, 1 μM dex, 1 μg/ml INS, and 1 μM rosiglitazone for 48 h two times. (G) Treatment with 1 μM dex and 1 μg/ml INS for 48 h followed by 0.5 mM IBMX treatment for 48 h. (H) Treatment with 0.5 mM IBMX and 1 μg/ml INS for 48 h followed by 1 μM dex treatment for 48 h.

this commitment state at the molecular level, we used genomewide microarrays to interrogate gene expression in 2-d confluent 3T3-L1 preadipocytes, with or without dex treatment. We found that dex treatment for 2 or 36 h significantly affected 94 and 163 genes, respectively, by more than twofold.

Next, we compared the expression profile of dex-primed preadipocytes with that from published data of preadipocytes treated with DIM for 4 d to induce full adipogenesis (Figure 3 and Supplemental Table 1; Burton *et al.*, 2004). We found that ~80% of the genes affected by dex treatment alone were also modulated by DIM treatment during the 4-d time course (Figure 3A). Additionally, cluster analysis revealed that the set of genes regulated by dex includes genes modulated throughout the 4-d DIM time course (Figure 3B). We then performed gene ontology analysis comparing the genes modulated by dex alone with the genes modulated by DIM, but not dex. Notably, dex selectively modulates the expression of genes that participate in extracellular matrix processes and the transforming growth factor-beta (TGFβ), WNT (wingless/Int), and MAP kinase pathways; in contrast, genes regulated by DIM, but not affected by dex alone, impact intracellular processes, mitochondrial function, lipid synthesis, glucose and NAD metabolism, oxidative phosphorylation, and the citrate cycle (Figure 3C). Thus, dex-primed preadipocytes express a genetic program distinct from that of adipocytes and appear to represent a discrete intermediate between the preadipocyte and the adipocyte.

Effect of Differentiation by Sequential Treatment with Dex and IBMX on the Metabolic Properties of Adipocytes

To further characterize the metabolic properties of preadipocytes treated sequentially with dex followed by IBMX and vice versa, we assessed in 3T3-L1 cells functional parameters characteristic of adipocytes: insulin-stimulated glucose uptake, lipolysis, and total triglyceride levels (Figure 4).

Adipocytes treated with insulin respond by increasing rates of glucose transport; thus, the amount of glucose internalized after insulin treatment is a measure of insulin sensitivity. We found that the insulin sensitivity of adipocytes generated by sequential treatment of 3T3-L1 preadipocytes with dex and IBMX was equal to that of DIM adipocytes. Cells treated with IBMX followed by dex behaved similar to control cells and did not increase their glucose uptake after insulin treatment (Figure 4A).

Adipocytes store energy as triglycerides in fat droplets. The energy stores can be mobilized in times of need by signals that increase lipolysis rates. At the organismal level the sympathomimetic system generates such signals by producing adrenergic stimuli. The beta-adrenergic agonist ISO can be used in cell culture to simulate these conditions; preadipocytes, unlike adipocytes, do not respond to ISO. Adipocytes differentiated by sequential treatment with dex and IBMX displayed basal lipolysis rates equivalent to DIM adipocytes (212 ± 5 vs. 212 ± 7 μmol of glycerol/h). DIM adipocytes increased their rates of lipolysis by 127 ± 15% above the basal rate, whereas dex-IBMX adipocytes increased their rates by 82 ± 2% above basal after ISO treatment, representing a significantly lower increase in lipolysis ($p = 1.7e\text{-}2$). Once again, cells treated with IBMX followed by dex did not differ from control preadipocytes (Figure 4B).

Measurement of total triglyceride levels showed that DIM adipocytes stored approximately four times more triglycerides than preadipocytes. Dex-IBMX adipocytes stored ~1.8-fold more triglycerides than preadipocytes. IBMX-dex–treated preadipocytes contained the same amount of triglycerides as control preadipocytes (Figure 4C). These data are consistent with the lower retention of Oil Red O by the dex-IBMX adipocytes compared with the DIM adipocytes.

These results revealed an unexpected interaction between the signaling pathways modulated by dex and IBMX as part of the DIM cocktail. In that context, dex and IBMX seem to act synergistically and are both required for robust adipogenesis. However, when dex and IBMX activities were temporally uncoupled, preadipocytes were able to detect the order in which these pathways signal and only differentiated if dex acted before IBMX. To investigate the mechanism by which preadipocytes distinguished between the different orders of exposure to dex and IBMX, we characterized the pattern of expression of some key adipogenic regulatory factors after sequential treatment.

Effect of Differentiation Mode on the Expression of Adipogenic Transcriptional Regulatory Factors

Treatment of preadipocytes with the DIM differentiation cocktail induces a cascade of transcription factors that is responsible for the initiation and establishment of the adipogenic cell fate. The initial step of the adipogenic transcriptional cascade is the transient induction of the transcriptional regulatory factors CCAAT/enhancer-binding protein

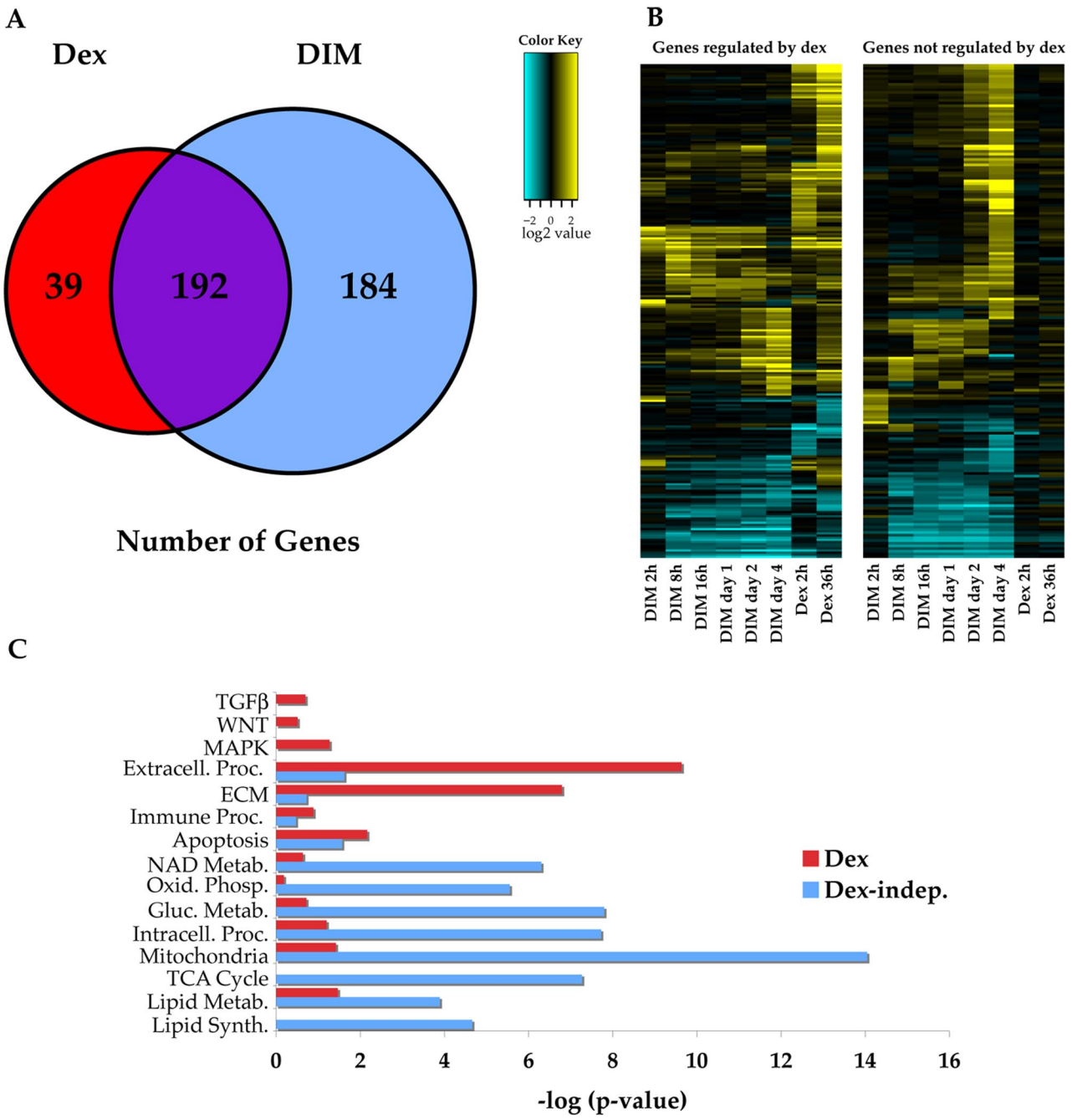

Figure 3. Expression profiles of dex-treated preadipocytes and DIM-induced adipogenesis. (A) Overlap of genes affected by dex treatment at 2 or 36 h (red) and genes affected during 4 d of DIM-induced adipogenesis (blue). (B) Hierarchical clustering of genes affected by dex (left) or those affected by DIM, but not dex (right). Genes (rows) were clustered using noncentered Pearson correlation distance and average linkage agglomeration. (C) The expression profile of dex treatment of preadipocytes at 2 or 36 h was compared with a published dataset of DIM-induced adipogenesis over 4 d (Burton *et al.*, 2004). p values of select gene ontology categories from DAVID 2008 (Dennis *et al.*, 2003) are shown for genes affected by dex (red) or those affected by DIM, but not dex (Dex-indep., blue).

beta and delta (C/EBPβ and C/EBPδ). Previous studies using 3T3-L1 cells have demonstrated that in the DIM cocktail dex is the main inducer of C/EBPδ, whereas IBMX is responsible for the induction of C/EBPβ. Next, C/EBPβ and C/EBPδ act together to activate expression of C/EBPα and peroxisome proliferator-activated receptor gamma (PPARγ). Various other transcription factors are known to modulate adipogenesis, but they all seem to act by modulating the expression of either PPARγ or of one of the C/EBPs (Farmer, 2006).

We used qPCR and immunoblotting to monitor the levels of C/EBPα, β, δ, and PPARγ at 2, 4, 6, 8, and 10 d after treatment with DIM, after sequential treatment with dex followed by IBMX or after sequential treatment with IBMX followed by dex (Figure 5). We sought to determine if the disparate differentiation outcomes induced by the two

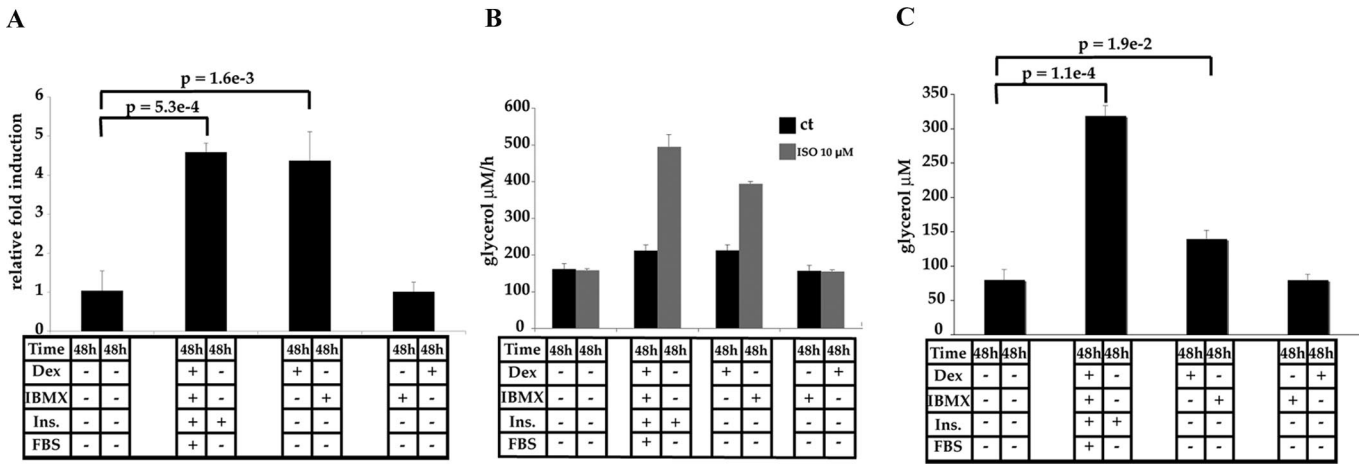

Figure 4. Effect of differentiation conditions on the metabolic properties of 3T3-L1 cells. 3T3-L1 preadipocytes on day 2 after confluence were treated with combinations of 0.5 mM IBMX, 1 μM dex, 1 μg/ml INS or 10% FBS. (A) Insulin-induced glucose uptake. Day 10 after treatment 3T3-L1 cells were treated with 10 μg/ml insulin for 10 min. Uptake of 2-DG was measured by scintillography. Data are means $\pm$ SD; n $\geq$ 3. (B) Isoproterenol-stimulated lipolysis. Day 10 after treatment 3T3-L1 cells were treated with 10 μM ISO for 3 h. Measurement of glycerol secretion in the medium was used to determine rate of ISO-induced lipolysis. Data are means $\pm$ SD of three independent experiments. (C) Triglyceride storage. Total triglyceride levels of day 10 after treatment 3T3-L1 cells were measured through an enzymatic colorimetric assay. Data are means $\pm$ SD of three independent experiments.

sequential treatments were reflective of differential patterns of expression of C/EBPα, β, δ, and PPARγ.

qPCR analysis revealed the following differences between sequential treatments and the standard, DIM-induced pattern of expression: 1) Treatment of 3T3-L1 preadipocytes with dex followed by IBMX transiently induced C/EBPδ on day 2 and then C/EBPβ on day 4; the pattern of expression of PPARγ and C/EBPα mRNAs was similar to DIM-treated cells (Figure 5A). 2) Treatment of 3T3-L1 preadipocytes with IBMX followed by dex transiently increased the levels of C/EBPβ mRNA by threefold on day 2; C/EBPδ expression was delayed, increasing above control levels only on day 6; PPARγ and C/EBPα mRNA levels were above control (3–13-fold) during days 4–10 (Figure 5A). Interestingly, despite induction of PPARγ and C/EBPα mRNAs, the IBMX-dex treatment did not promote substantial adipogenesis.

Immunoblot analysis revealed that preadipocytes treated with dex for 48 h followed by IBMX for 48 h displayed an increase in C/EBPδ levels with dex treatment at day 2 followed by a decline in protein levels after IBMX treatment on day 4. C/EBPβ reached levels above untreated cells on day 4 after treatment and decreased after day 6. C/EBPα and PPARγ protein levels started to increase on day 4 and reached levels equivalent to DIM-treated cells on day 6 after treatment (Figure 5B).

Treatment of 3T3-L1 preadipocytes with IBMX followed by dex led to increases in the protein levels of C/EBPβ and C/EBPδ relative to untreated cells. C/EBPβ reached its highest levels on day 6 after treatment. C/EBPδ levels surpassed untreated cells on day 6 and increased slightly thereafter. Notably, the increases in C/EBPβ and C/EBPδ levels were not associated with increased protein levels of C/EBPα or PPARγ. This may indicate that a threshold level of C/EBPβ and C/EBPδ was required to achieve C/EBPα and PPARγ expression, and subsequent adipogenesis.

Pref-1 Is a Sensor of Dex and IBMX Signaling

Pref-1 is related to the Notch/Delta/Serrate family of secreted epidermal growth factor-like repeat-containing proteins and is one of the most highly expressed mRNAs in 3T3-L1 preadipocytes. During differentiation induced by the DIM cocktail, Pref-1 levels decline dramatically and it has been demonstrated that Pref-1 is an inhibitor of adipogenesis in vitro and in vivo (Wang *et al.*, 2006). Forced expression of Pref-1 in preadipocytes inhibits differentiation, while knockdown enhances it. Moreover, mice overexpressing the soluble form of Pref-1 display decreased adipose tissue mass, whereas Pref-1 knockout mice possess increased adipose tissue mass. The down-regulation of Pref-1 during DIM-induced adipogenesis is conferred by dex, which inhibits Pref-1 transcription in a dose- and time-dependent manner that correlates with glucocorticoid-promoted differentiation (Smas *et al.*, 1999). We hypothesized that this repression of Pref-1 by dex may be somehow affected by IBMX.

To test our hypothesis we used qPCR and immunoblots to monitor mRNA and protein levels of Pref-1 after treating 3T3-L1 preadipocytes with the DIM cocktail, dex followed by IBMX, and IBMX followed by dex. We found that treatment of 3T3-L1 preadipocytes with dex followed by IBMX or with the DIM cocktail decreased Pref-1 mRNA levels by up to 10-fold relative to control cells. In contrast, treatment with IBMX followed by dex was relatively ineffective at repressing Pref-1 (Figure 6A). Pref-1 protein levels paralleled the Pref-1 mRNA findings. Treatment with dex followed by IBMX or with the DIM cocktail reduced Pref-1 protein to almost undetectable levels. 3T3-L1 preadipocytes treated with IBMX-dex maintained levels of Pref-1 expression similar to untreated cells, despite being slightly repressed on day 4 of IBMX-dex treatment (Figure 6B).

DISCUSSION

The steps involved in adipocyte formation have remained unresolved for the past two decades. To gain insight into this process, we used a reductionist approach with two related aims: first, to test the hypothesis that individual components of the DIM cocktail regulate discrete commitment states in the progression from preadipocyte to adipocyte; second, to assess at the molecular level the contributions of the

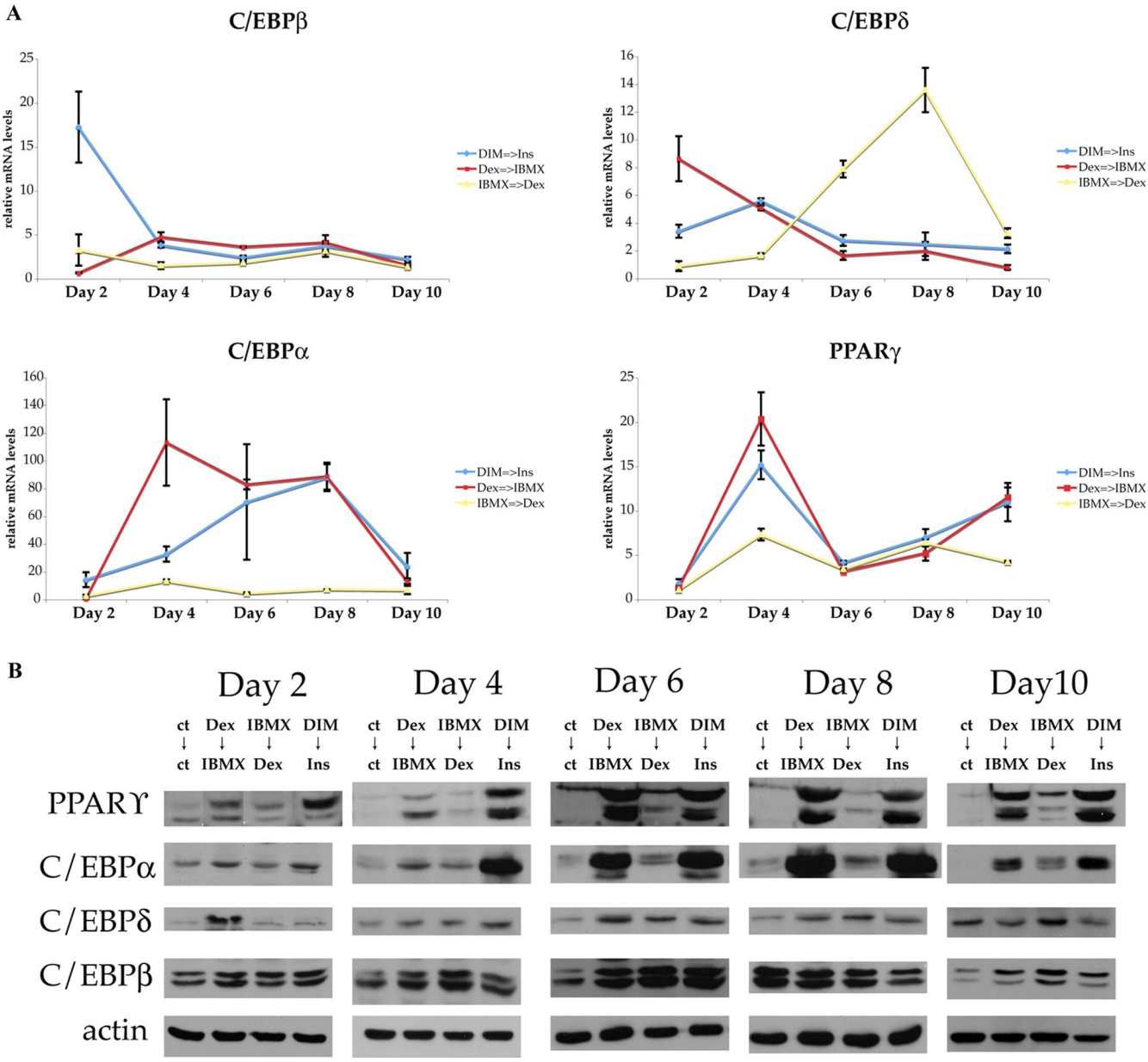

Figure 5. Levels of adipogenic transcription factors during differentiation induced by sequential treatment with dex and IBMX. (A) RNA was extracted from 3T3-L1 cells 2, 4, 6, 8, and 10 d after induction of differentiation by treatment with the DIM cocktail, dex for 48 h followed by IBMX for 48 h, and IBMX for 48 h followed by dex for 48 h. mRNA levels were quantified by quantitative real-time PCR. Data were normalized relative to untreated cells mRNA levels and show mean ± SD. (B) Protein lysates were prepared from 3T3-L1 cells 2, 4, 6, 8, and 10 d after induction of differentiation by treatment with the DIM cocktail, dex for 48 h followed by IBMX for 48 h, and IBMX for 48 h followed by dex for 48 h. Proteins were separated by SDS-page, transferred, and immunoblotted with specific primary antibodies directed against PPARγ, C/EBPα, C/EBPδ, and C/EBPβ, or β-actin.

individual components to adipogenesis. Through this approach we determined conditions for differentiation of 3T3-L1 preadipocytes that are independent of insulin addition, as previously demonstrated (Schmidt *et al.*, 1990; Liu *et al.*, 2005), or of shifting to growth medium supplemented with FBS. Our approach yielded a simpler, more direct model for inducible adipogenesis. Differentiation can be divided into two distinct stages induced by two signaling pathways acting sequentially, but noncommutatively. The initial phase is driven by glucocorticoid signaling and is followed by a second phase driven by cAMP signaling. The significance of the relationship between dex and IBMX in 3T3-L1 cells was recapitulated in C3H10T1/2 cells and in primary MSCs.

The current models of fat ontogenesis do not seem to account for the diversity of adipocyte phenotypes observed in vivo and are simplistic compared with the much better understood hematopoietic system (Schmidt *et al.*, 1990; Gesta *et al.*, 2007). In our experiments, we isolated the actions of glucocorticoid signaling during adipogenesis and found that pretreatment with dex primes preadipocytes to respond to IBMX and induces a gene expression profile intermediary between that of preadipocytes and adipocytes. Thus, glu-

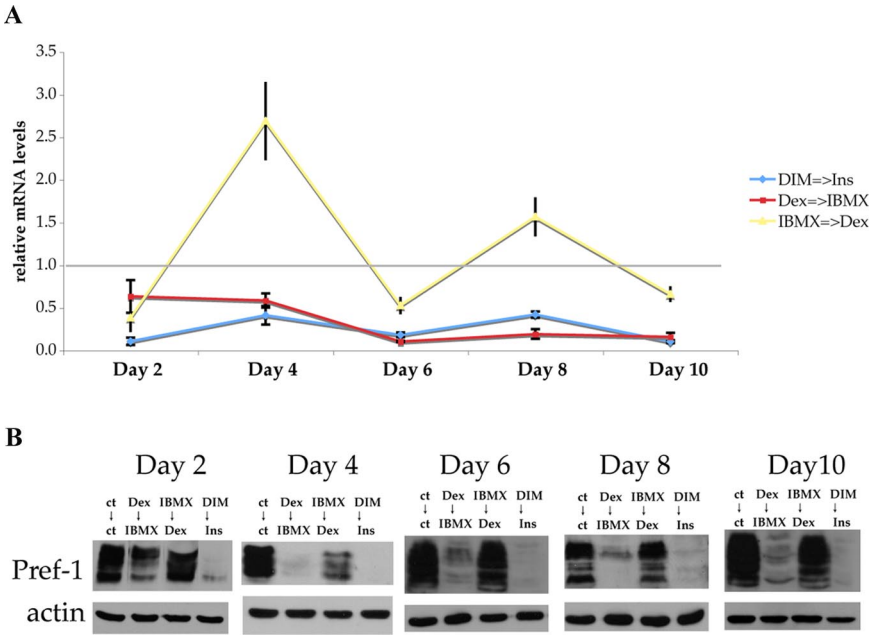

Figure 6. Effect of differentiation condition on the levels of Pref-1. (A) RNA was extracted from 3T3-L1 cells 2, 4, 6, 8, and 10 d after induction of differentiation by treatment with the DIM cocktail, dex for 48 h followed by IBMX for 48 h and IBMX for 48 h followed by dex for 48 h. mRNA levels were quantified by quantitative real-time PCR. Data were normalized relative to untreated cells mRNA levels and show mean ± SD. (B) Protein lysates were prepared from 3T3-L1 cells 2, 4, 6, 8, and 10 d after induction of differentiation by treatment with the DIM cocktail, dex for 48 h followed by IBMX for 48 h, and IBMX for 48 h followed by dex for 48 h. Proteins were separated by SDS-page, transferred, and immunoblotted with specific primary antibodies directed against Pref-1 or β-actin.

cocorticoid signaling appears to define a novel commitment state, the dex-primed preadipocyte. Although the physiological relevance of these findings remains to be determined, it is interesting that patients exposed to excess glucocorticoids present with expansion of a subset of fat depots. Conceivably, certain adipose niches (e.g., visceral fat depot) may be permissive for differentiation of dex-primed preadipocytes, whereas other fat depots may be insensitive to glucocorticoid-induced adipogenesis because they lack the permissive signals that advance dex-primed preadipocytes through the adipogenic program.

In contrast to the outcomes of dex pretreatment of preadipocytes, the increased cAMP signaling resulting from IBMX pretreatment of those cells results in a failure to differentiate upon subsequent dex treatment; these cells are also partially resistant to differentiation induced by the DIM cocktail. Recently, Madsen *et al.* (2008) linked increased cAMP signaling in mouse liver and adipose tissues, induced by high-protein diet, to prevention of polyunsaturated fatty acid–induced adipogenesis and obesity. These findings indicate that, in contrast to glucocorticoids, stimulation of cAMP signaling in preadipocytes fails to induce progression toward the adipocyte fate. On the contrary, it seems that IBMX drives preadipocytes toward a state that is off of the adipogenic pathway, but that does not represent a terminal differentiation fate. Accordingly, we found that IBMX-pretreated preadipocytes can differentiate into adipocytes if treated with dex for 48 h followed by IBMX for another 48 h (Supplemental Figure S1). Hence, dex signaling acts dominantly to cAMP signaling to return IBMX-treated preadipocytes to the adipogenesis pathway.

Thus, we suggest that glucocorticoids and cAMP appear to regulate adipogenesis independently by directing preadipocytes toward two cellular states. Dex-primed preadipocytes are on-pathway toward the adipocyte fate; IBMX-treated preadipocytes are off-pathway and differentiate efficiently only if brought back to the adipogenic pathway by dex signaling. These two observations suggest a simple way by which adipogenesis can be spatially and temporally compartmentalized during development and normal adult life and in disease states. Specifically, preadipocytes may integrate order, intensity (e.g., dose of glucocorticoid), and duration of adipogenic signals to adopt distinct cellular states, along an adipogenesis axis, that differ in their sensitivity to further stimulation.

The insulin sensitivity of adipocytes differentiated by treatment with dex followed by IBMX was equivalent to DIM-differentiated adipocytes (Figure 4A). Accordingly, the two types of adipocytes expressed similar mRNA levels of the glucose transporter GLUT4 (Supplemental Figure S3A). Dex-IBMX adipocytes, however, were less sensitive to induction of lipolysis by the β-adrenergic agonist ISO when compared with DIM-differentiated adipocytes (Figure 4B). Interestingly, we found that this phenotype correlated with decreased levels of the lipid droplet protein perilipin A on dex-IBMX adipocytes relative to DIM-differentiated adipocytes (Supplemental Figure S3B). Perilipin A is thought to influence adipocyte lipolysis by a mechanism that is dependent on its expression levels and phosphorylation state (Brasaemle, 2007). When unphosphorylated, perilipin A protects lipid droplets from the activity of cellular lipases and promotes triglyceride storage. Upon ISO stimulation perilipin A phosphorylation is required for full induction of lipolysis and promotes localization of hormone-sensitive lipase to the surface of lipid droplets. Indeed, adipocytes derived from perilipin A null mice display slightly elevated basal lipolysis, but dramatically decreased ISO-stimulated lipolysis (Tansey *et al.*, 2001). Thus, the lower levels of perilipin A on dex-IBMX adipocytes may underlie the decrease in ISO-stimulated lipolysis, but unchanged basal lipolysis rates when compared with DIM-adipocytes (Figure 4B and Supplemental Figure S3B).

In addition to being less responsive to the lipolytic effect of ISO, dex-IBMX 3T3-L1 adipocytes stored less triglyceride (Figure 4C). The triglyceride storage phenotype could reflect the absence of insulin-dependent activation of cyclic AMP response element binding protein (CREB), which in turn stimulates triglyceride accumulation in 3T3-L1 adipocytes (Klemm *et al.*, 2001; Vankoningsloo *et al.*, 2006). Additionally, it is consistent with clinical studies showing that excess circulating insulin levels are associated with larger subcutaneous adipocytes. These results indicate that selected aspects of adipocyte metabolic function can be tuned by the mode

of differentiation to which preadipocytes are subjected. In an interesting parallel, the human visceral fat depot displays higher rates of catecholamine-induced lipolysis relative to the subcutaneous white fat depots (Arner, 1999, 2001). The similarities between our cell culture results and the diversity of adipocytes in human subjects suggest a clear path for discerning the mechanisms that contribute to the final metabolic phenotype of adipose tissue. Importantly, the differences in expression of perilipin A suggest that its regulation might be part of the mechanism through which adipocyte metabolic diversity is generated.

We applied a candidate approach to infer the mechanism by which the order of exposure to dex and IBMX alters the adipogenesis signal. We found that relative to DIM treatment, IBMX-dex treated cells displayed delayed expression of C/EBPδ and did not substantially increase the protein levels of C/EBPα and PPARγ. Our findings suggest that early expression of C/EBPδ is required for efficient induction of C/EBPα and PPARγ. To explore additional mechanisms underlying the failure of IBMX-dex treatment to induce differentiation, we monitored Pref-1, whose repression by glucocorticoids is necessary for efficient adipogenesis of 3T3-L1 preadipocytes. We found that dex-IBMX treatment indeed represses Pref-1, whereas pretreatment with IBMX prevents stable repression of Pref-1 by dex. These results suggest a mechanism by which preadipocytes sense the order of exposure to dex and IBMX and underscore a role of Pref-1 as a molecular gatekeeper of adipogenesis. In related studies, Feldman *et al.* (2006) identified an adipogenesis role for a glucocorticoid receptor target gene, the TGFβ family member myostatin (MSTN). Remarkably, C3H10T1/2 adipocytes differentiated by substitution of dex with MSTN and adipocytes of mice expressing MSTN in adipose tissue are smaller and more insulin sensitive and seem to be immature when compared with wild-type adipocytes. It will be interesting to determine the relationship of those "myostatin adipocytes" to the dex-primed preadipocytes described in our work.

In summary, by temporally uncoupling the signals that comprise the DIM cocktail, we discovered complex interactions of dex and IBMX during adipogenesis in cell culture, which may enrich our understanding of the process and its regulation as played out in intact mammalian organisms. Our results, and those of Feldman *et al.* (2006), imply that an array of intermediate cell types, perhaps reminiscent of those known in hematopoiesis, may punctuate cell fate pathways radiating from mesenchymal stem cells, and in particular proceeding toward mature adipocytes. The distinct metabolic capabilities of dex-IBMX adipocytes compared with DIM adipocytes may reflect a mechanism by which adipogenesis can be fine-tuned spatially, temporally, and functionally to generate the diversity of adipocyte phenotypes described in vivo. In this context, it is intriguing that Pref-1 may, under certain circumstances, act as a sensor of glucocorticoid and cyclic AMP activities, ensuring that preadipocytes advance to differentiation only if a predetermined series of signaling events occurs in the correct order.

ACKNOWLEDGMENTS

We thank the members of the Yamamoto lab for discussions and reagents, and Kaveh Ashrafi, Brian Black, Eric Bolton, Brian Feldman, Tony Gerber, Marlisa Pillsbury, and Wally Wang for insightful comments on the manuscript. Primary mouse mesenchymal stem cells were generously provided by Brian Feldman (Department of Pediatrics, University of California, San Francisco). This work was supported by predoctoral fellowship 0515044Y and 0715058Y of the American Heart Association to C.P., institutional training grant T32GM07810 from the National Institutes of Health (NIH) to J.T.H., and NIH, National Cancer Institute Grant CA020535 to K.R.Y.

REFERENCES

Arner, P. (1999). Catecholamine-induced lipolysis in obesity. Int. J. Obes. Relat. Metab. Disord. *23*(Suppl 1), 10–13.

Arner, P. (2001). Regional differences in protein production by human adipose tissue. Biochem. Soc. Trans. *29*, 72–75.

Bolstad, B. M., Irizarry, R. A., Astrand, M., and Speed, T. P. (2003). A comparison of normalization methods for high density oligonucleotide array data based on variance and bias. Bioinformatics *19*, 185–193.

Brasaemle, D. L. (2007). Thematic review series: adipocyte biology. The perilipin family of structural lipid droplet proteins: stabilization of lipid droplets and control of lipolysis. J. Lipid Res. *48*, 2547–2559.

Burton, G. R., Nagarajan, R., Peterson, C. A., and McGehee, R. E., Jr. (2004). Microarray analysis of differentiation-specific gene expression during 3T3–L1 adipogenesis. Gene *329*, 167–185.

Dennis, G., Jr., Sherman, B. T., Hosack, D. A., Yang, J., Gao, W., Lane, H. C., and Lempicki, R. A. (2003). DAVID: Database for Annotation, Visualization, and Integrated Discovery. Genome Biol. *4*, P3.

Farmer, S. R. (2006). Transcriptional control of adipocyte formation. Cell Metab. *4*, 263–273.

Feldman, B. J., Streeper, R. S., Farese, R. V., Jr., and Yamamoto, K. R. (2006). Myostatin modulates adipogenesis to generate adipocytes with favorable metabolic effects. Proc. Natl. Acad. Sci. USA *103*, 15675–15680.

Fujikura, J., Fujimoto, M., Yasue, S., Noguchi, M., Masuzaki, H., Hosoda, K., Tachibana, T., Sugihara, H., and Nakao, K. (2005). Insulin-induced lipohypertrophy: report of a case with histopathology. Endocr. J. *52*, 623–628.

Funahashi, T., and Matsuzawa, Y. (2007). Metabolic syndrome: clinical concept and molecular basis. Ann. Med. *39*, 482–494.

Gentleman, R. C. *et al.* (2004). Bioconductor: open software development for computational biology and bioinformatics. Genome Biol. *5*, R80.

Gesta, S., Bluher, M., Yamamoto, Y., Norris, A. W., Berndt, J., Kralisch, S., Boucher, J., Lewis, C., and Kahn, C. R. (2006). Evidence for a role of developmental genes in the origin of obesity and body fat distribution. Proc. Natl. Acad. Sci. USA *103*, 6676–6681.

Gesta, S., Tseng, Y. H., and Kahn, C. R. (2007). Developmental origin of fat: tracking obesity to its source. Cell *131*, 242–256.

Klemm, D. J., Leitner, J. W., Watson, P., Nesterova, A., Reusch, J. E., Goalstone, M. L., and Draznin, B. (2001). Insulin-induced adipocyte differentiation. Activation of CREB rescues adipogenesis from the arrest caused by inhibition of prenylation. J. Biol. Chem. *276*, 28430–28435.

Kondo, M., Wagers, A. J., Manz, M. G., Prohaska, S. S., Scherer, D. C., Beilhack, G. F., Shizuru, J. A., and Weissman, I. L. (2003). Biology of hematopoietic stem cells and progenitors: implications for clinical application. Annu. Rev. Immunol. *21*, 759–806.

Liu, J., DeYoung, S. M., Zhang, M., Zhang, M., Cheng, A., and Saltiel, A. R. (2005). Changes in integrin expression during adipocyte differentiation. Cell Metab. *2*, 165–177.

Madsen, L. et al. (2008). cAMP-dependent Signaling Regulates the Adipogenic Effect of n-6 Polyunsaturated Fatty Acids. J. Biol. Chem. *283*, 7196–7205.

Ogden, C. L., Yanovski, S. Z., Carroll, M. D., and Flegal, K. M. (2007). The epidemiology of obesity. Gastroenterology *132*, 2087–2102.

Otto, T. C., and Lane, M. D. (2005). Adipose development: from stem cell to adipocyte. Crit. Rev. Biochem. Mol. Biol. *40*, 229–242.

Peinnequin, A., Mouret, C., Birot, O., Alonso, A., Mathieu, J., Clarencon, D., Agay, D., Chancerelle, Y., and Multon, E. (2004). Rat pro-inflammatory cytokine and cytokine related mRNA quantification by real-time polymerase chain reaction using SYBR green. BMC Immunol. *5*, 3.

Rockall, A. G., Sohaib, S. A., Evans, D., Kaltsas, G., Isidori, A. M., Monson, J. P., Besser, G. M., Grossman, A. B., and Reznek, R. H. (2003). Computed tomography assessment of fat distribution in male and female patients with Cushing's syndrome. Eur. J. Endocrinol. *149*, 561–567.

Schmidt, W., Poll-Jordan, G., and Loffler, G. (1990). Adipose conversion of 3T3–L1 cells in a serum-free culture system depends on epidermal growth factor, insulin-like growth factor I, corticosterone, and cyclic AMP. J. Biol. Chem. *265*, 15489–15495.

Smas, C. M., Chen, L., Zhao, L., Latasa, M. J., and Sul, H. S. (1999). Transcriptional repression of pref-1 by glucocorticoids promotes 3T3–L1 adipocyte differentiation. J. Biol. Chem. *274*, 12632–12641.

Smyth, G. K. (2004). Linear models and empirical bayes methods for assessing differential expression in microarray experiments. Stat. Appl. Genet. Mol. Biol. *3*, Article 3.

Smyth, G. K., and Speed, T. (2003). Normalization of cDNA microarray data. Methods *31*, 265–273.

Tansey, J. T. *et al.* (2001). Perilipin ablation results in a lean mouse with aberrant adipocyte lipolysis, enhanced leptin production, and resistance to diet-induced obesity. Proc. Natl. Acad. Sci. USA *98*, 6494–6499.

Tchkonia, T. et al. (2007). Identification of depot-specific human fat cell progenitors through distinct expression profiles and developmental gene patterns. Am. J. Physiol. Endocrinol. Metab. *292*, E298–E307.

Vankoningsloo, S., De Pauw, A., Houbion, A., Tejerina, S., Demazy, C., de Longueville, F., Bertholet, V., Renard, P., Remacle, J., Holvoet, P., Raes, M., and Arnould, T. (2006). CREB activation induced by mitochondrial dysfunction triggers triglyceride accumulation in 3T3–L1 preadipocytes. J. Cell Sci. *119*, 1266–1282.

Wang, Y., Kim, K. A., Kim, J. H., and Sul, H. S. (2006). Pref-1, a preadipocyte secreted factor that inhibits adipogenesis. J. Nutr. *136*, 2953–2956.